frontiers | Frontiers in Marine Science

TYPE Brief Research Report
PUBLISHED 25 August 2022
DOI 10.3389/fmars.2022.975062

OPEN ACCESS

EDITED BY
Daniel Rittschof,
Duke University, United States

REVIEWED BY
Michael Schultz,
United States Naval Academy, United States
Michael L. Fine,
Virginia Commonwealth University, United States

*CORRESPONDENCE
Molly K. Gabler-Smith
mollygablersmith@gmail.com

SPECIALTY SECTION
This article was submitted to Marine Biotechnology and Bioproducts, a section of the journal Frontiers in Marine Science

RECEIVED 21 June 2022
ACCEPTED 08 August 2022
PUBLISHED 25 August 2022

CITATION
Gabler-Smith MK and Lauder GV (2022) Ridges and riblets: Shark skin surfaces versus biomimetic models. *Front. Mar. Sci.* 9:975062. doi: 10.3389/fmars.2022.975062

Ridges and riblets: Shark skin surfaces versus biomimetic models

Molly K. Gabler-Smith* and George V. Lauder

Department of Organismic and Evolutionary Biology, Harvard University, Cambridge, MA, United States

Shark skin has been an inspiration for biomimetic materials and structures due to its role in reducing drag and enhancing thrust, properties believed to be due to the textured surface composed of ridges on the surface of individual tooth-like scales (denticles). Attempts to replicate the hydrodynamic performance of shark skin have involved manufacturing both engineered riblets and fabrics with textured surfaces. However, there are no studies that compare the surface ornamentation of shark denticles to bioinspired materials. Using three-dimensional surface profilometry we analyzed the cross-sectional profile of the surface of shark denticles at two locations on 17 species and compared these data to values obtained from engineered structures (e.g., riblets) and competition swimsuits that are often proposed as having a comparable surface texture to shark skin. Of the variables measured, crown aspect ratio ($p = 0.007$), ridge height, ridge spacing, ridge aspect ratio, and ridge bumpiness (all $p < 0.001$) differed among the three materials. Overall, engineered riblet surfaces were very different than biological shark skin. Some of the competition swimsuit materials were more shark-like, with the fabric texture having similar height variation, but with irregular ridge spacing. Cross-sectional profile, which includes pathlength and aspect ratio in addition to ridge spacing and height, is an important feature of the skin's surface, affecting water flow over the individual denticles, and future research will address these parameters. Quantitative 3D analysis of the surface of real shark denticle ridges enables the design of more biomimetic engineered shark skin surfaces.

KEYWORDS

sharks, dermal denticles, locomotion, riblets, morphology, biomimetics, skin

Introduction

Over the past century, many marine organisms have served as a source for the design of bioinspired robots and other structures. For example, designs of grasping devices have been inspired by octopus arms and suckers (Laschi et al., 2009; Margheri et al., 2012; Xie et al., 2020), digging mechanisms by clams (Winter and Hosoi, 2011), and swimming

robotic systems have been produced based on principles of tuna locomotion (Zhu et al., 2019; White et al., 2021). Sharks have been a particularly important group stimulating the manufacture of biomimetic materials, specifically due to the unique structures on their skin: dermal scales or denticles. Shark denticles are tooth-like structures, cover the surface of all shark species, and vary in their shape, size, and surface characteristics including the presence/absence of ridges, ridge height, and ridge spacing (Rief, 1985; Castro, 2011; Motta et al., 2012; Ankhelyi et al., 2018; Popp et al., 2020; Gabler-Smith et al., 2021). Although dermal denticles likely have various functions (e.g., abrasion reduction, parasite deterrence, protection from predators), the ability of these microscopic structures to reduce drag and enhance thrust during aquatic locomotion has been of considerable interest in the biomimetic and bioinspiration community for years (Bechert et al., 1985; García-Mayoral and Jiménez, 2011; Wen et al., 2014; Domel et al., 2018a; Suprapaneni et al., 2022). If inspiration from the design of shark skin can be applied to fabricated and engineered materials, then application of such bioinspired materials to the hulls of both surface and underwater vehicles could assist in reducing the energetic cost of moving through water.

But how well do current engineered or fabricated materials match the characteristics of shark skin? Fabric designed for competition swimsuits has achieved some notoriety by increasing the speed of swimmers (Takagi and Sanders, 2000; Hutchinson, 2008; Oeffner and Lauder, 2012), and shark skin-inspired engineered riblet surfaces have been applied to wind turbines (Chamorro et al., 2013; Sareen et al., 2014; Leitl et al., 2020), and tested for drag reduction properties (Bechert et al., 2000; Zhao et al., 2012; Ibrahim et al., 2018). Do these current applications, generally inspired by shark skin, possess quantitatively accurate three-dimensional (3D) surface characteristics that match shark skin? Previous efforts to compare engineered surfaces to shark skin have been largely qualitative, and such comparisons have been limited due to the lack of information on the 3D profiles of shark skin denticle surfaces (see Wainwright et al., 2017; Ankhelyi et al., 2018). Scanning electron microscopy (SEM) is the technique most often used for imaging shark skin, but SEM images do not generally provide information on height variation across the denticle surface and on the shape and distribution of the longitudinal ridges that characterize denticle crown surfaces. Recently, 3D profilometry techniques have been applied to image the surface of biological materials (Wainwright et al., 2017; Wainwright and Lauder, 2018; Wainwright et al., 2019), allowing the measurement of shark denticle ridge heights, as well as profiles of ridges across the shark skin surface. Therefore, the goals of this paper are: (1) to determine if there is a difference in denticle surface microstructure between two locations within individual sharks: the midbody and tail regions; (2) to assess the extent to which cross-sectional profiles of denticle surfaces differ among sharks with differing ecological habitats; and (3) to quantitatively compare how surface ornamentation and microstructure of engineered riblets and competition swimsuit materials compare to biological denticles.

Methods

Material and skin sampling

Biological data were collected from 17 species of sharks that were either preserved specimens from the Museum of Comparative Zoology Ichthyology Collection or freshly frozen material. As shark denticles are hard tooth-like structures, we anticipate no differences in surface topography between tissue that was preserved in alcohol or freshly frozen: the effects of freezing or preservation on different skin regions within species would also not be a concern (see Wainwright et al., 2017; Gabler-Smith et al., 2021). There were two regions of interest: (1) skin from the midbody under the first dorsal fin, and (2) skin from the midcaudal fin region in the center of the tail surface (not from the leading or trailing edges). Additionally, species were grouped into broad habitat categories for comparison (refer to Table S1 for groupings and Gabler-Smith et al., 2021 for further information on ecological groupings of shark species). A number of engineered riblet materials and competition swimsuits were available from our previous research (Oeffner and Lauder, 2012; Wen et al., 2014; Wainwright and Lauder, 2016; Domel et al., 2018a; Domel et al., 2018b; Popp et al., 2020) and were imaged using surface profilometry (see Wainwright et al., 2017). In addition, data on riblet spacing and height for shark-inspired engineering materials or computational studies of riblet function were available from several publications (Table S2) and these data were included in the comparative analysis.

Surface profilometry

Individual denticles, or denticle-like structures from biological, engineered riblets, and swimsuit materials were examined using gel-based profilometry to image surface topography (Wainwright et al., 2017). This technique has been recently used to image the surfaces of fish, both preserved and live, as well as riblet materials and other fabricated materials (Wainwright et al., 2017; Domel et al., 2018b; Wainwright and Lauder, 2018; Popp et al., 2020). Gel-based profilometry works by pressing a clear elastomer gel with a painted bottom surface onto a region of interest and taking stereophotographs of the surface of the gel using different illumination angles. The stereophotographs are then reconstructed into 3D topographic surfaces from which various measurements can be collected (Wainwright and Lauder, 2016; Wainwright et al., 2017). From these 3D surfaces, we measured denticle crown aspect ratio (length/height), ridge spacing (ridge-to-ridge distance), and

ridge height (trough-to-peak height) from three denticles (Figures 1A, B), riblets, or ridge-like structures from the competition swimsuit materials. These measurements were used to calculate ridge aspect ratio (ridge height/ridge spacing) and crown bumpiness (ridge height/crown width).

Statistics

Paired t-tests were used to detect differences between the two locations within individuals (mid-body versus tail) in measured variables on shark skin. Data were pooled by ecological habitat (benthic, demersal, and pelagic) and analysis of variance (ANOVA) was used to determine if there were differences among habitats in measured variables. Data were also pooled by surface type (biological, engineered, or swimsuit). However, because the data were not normally distributed, non-parametric Kruskal-Wallis tests were used to determine differences in measured variables. Bonferroni *post hoc* tests were performed upon significant ANOVA and Kruskall-Wallis results to determine which surfaces were different from each other. Data were analyzed using the statistical software R (ver. 4.0.1, R Foundation for Statistical Computing, Vienna, Austria; R Core Team, 2020). All analyses were conducted with $\alpha = 0.05$.

Results

All surfaces imaged in this study had ridges present (Figure 2), with the exception of the angelshark (Table S1), which has skin with individual thorn-like denticles lacking ridges. All other shark species had denticles with well-defined, regularly spaced, ridges on their crown surfaces (Figures 2A, B). Profiles across the denticle surface show distinct ridges varying in height from 2.9 to 25.7 μm and ridge spacing between adjacent peaks from 29.6 to 151.7 μm among the sharks sampled. Competition swimsuit fabrics (Figures 2C, D) displayed much more irregular surface profiles with less distinct ridge peaks that ranged in height from 3.7 to 87.6 μm. Profiles across individual fabric surface elements projecting from the surface (the closest equivalent to denticle ridges) did not show distinct riblet patterns, but the magnitude of surface variation approached that of shark denticles (Figure 2D). 3D-printed shark denticles (Domel et al., 2018b) revealed a shark-like ridge pattern but with many fewer ridges that are much larger in height than those of sharks (Figure 2E).

Some measured variables differed between the midbody and midcaudal locations within individual sharks. Mean denticle crown width was larger at the midbody location (mean 374.7 ± 49.8 μm) compared to tail surfaces (mean 322.6 ± 43.6 μm, Table S1, Paired t-test: $p = 0.009$). Mean denticle crown aspect ratio was smaller at the midbody location (mean 1.3 ± 0.1) compared to the midcaudal (mean 1.5 ± 0.1, Table S1, Paired t-test: $p < 0.001$), suggesting that midbody denticles are squatter and squarer compared to those on the tail, which are more triangular. Due to some statistical differences between the two locations, both values were used in subsequent analyses.

Denticle features also differed when shark species were grouped according to habitat category (e.g., benthic, demersal, pelagic; Figures 3A; Figure S1, Table S1). Denticle crown width was higher in benthic species (mean 371.1 ± 33.0 μm, ANOVA: $p = 0.01$) compared to pelagic (mean 212.7 ±17.5 μm, Bonferroni: $p = 0.009$) but not demersal species (mean 331.6 ± 63.9 μm, Bonferroni: $p = 1.0$, demersal-pelagic $p = 0.4$). Crown length was also higher in benthic species (mean 548.2 ± 51.7 μm, ANOVA: $p = 0.002$) compared to pelagic (mean 252.9 ± 22.2 μm, Bonferroni: $p = 0.001$) but not demersal species (mean 383.9 ± 78.7 μm, Bonferroni: $p = 0.8$, demersal-pelagic $p = 0.4$). Crown aspect ratio was also

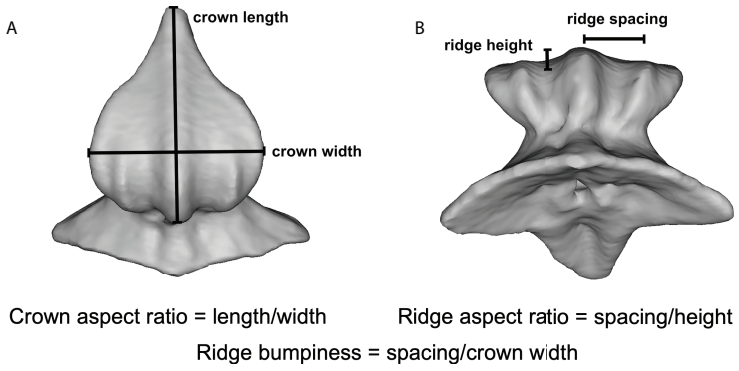

FIGURE 1
μCT images showing denticle and ridge measurements from a single leopard shark (*Triakis semifasciata*) denticle. **(A)** Dorsal view of denticle showing crown length and width measurements, and **(B)** view of the anterior denticle surface showing measured ridge height and spacing. Definitions of other calculated variables (i.e., crown aspect ratio, ridge aspect ratio, and ridge bumpiness) are given in the text.

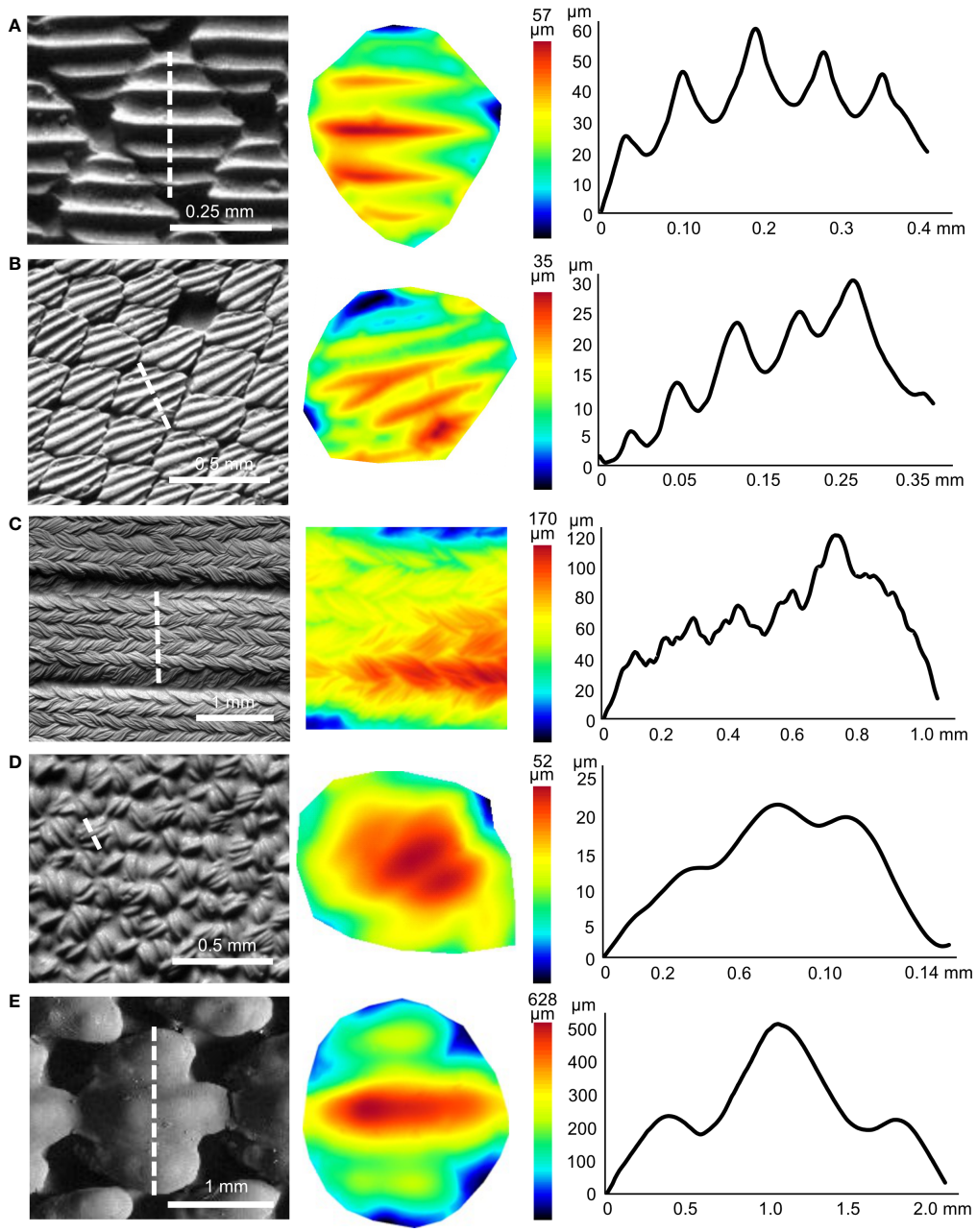

FIGURE 2
Three-dimensional surface structure for different shark skin and material samples. **(A)** Atlantic sharpnose shark (midbody), **(B)** Atlantic sharpnose shark (midtail), **(C)** Speedo® FS Fastskin II swimsuit, **(D)** Speedo Lzr® Racer Elite 2 swimsuit and **(E)** shark-inspired engineered surface (Domel et al., 2018b). Greyscale images from surface profilometry in the left column, with the white dotted line indicating the extracted profile. The center column shows topographic images (anterior to left) corresponding to the individual denticle or denticle-like structure from the left column, with color indicating surface height. The right column shows height profiles from the dotted lines in the left column images. Note that the y- and x-axes in the right column profiles are different for each image.

higher in benthic species (mean 1.5 ± 0.1, ANOVA: $p = 0.003$) compared to demersal (mean 1.1 ± 0.1, Bonferroni: $p = 0.03$) and pelagic species (mean 1.2 ± 0.1, Figure 3A, Bonferroni: $p = 0.01$). There was no difference in crown aspect ratio between demersal and pelagic species (Bonferroni: $p = 1.0$).

There were also considerable differences in the surface characteristics among the three classes of materials imaged. Crown aspect ratio differed among the materials (Kruskal-Wallis: $p = 0.007$): the engineered material (mean 1.1 ± 0.1) had a lower mean aspect ratio compared to the biological shark skin

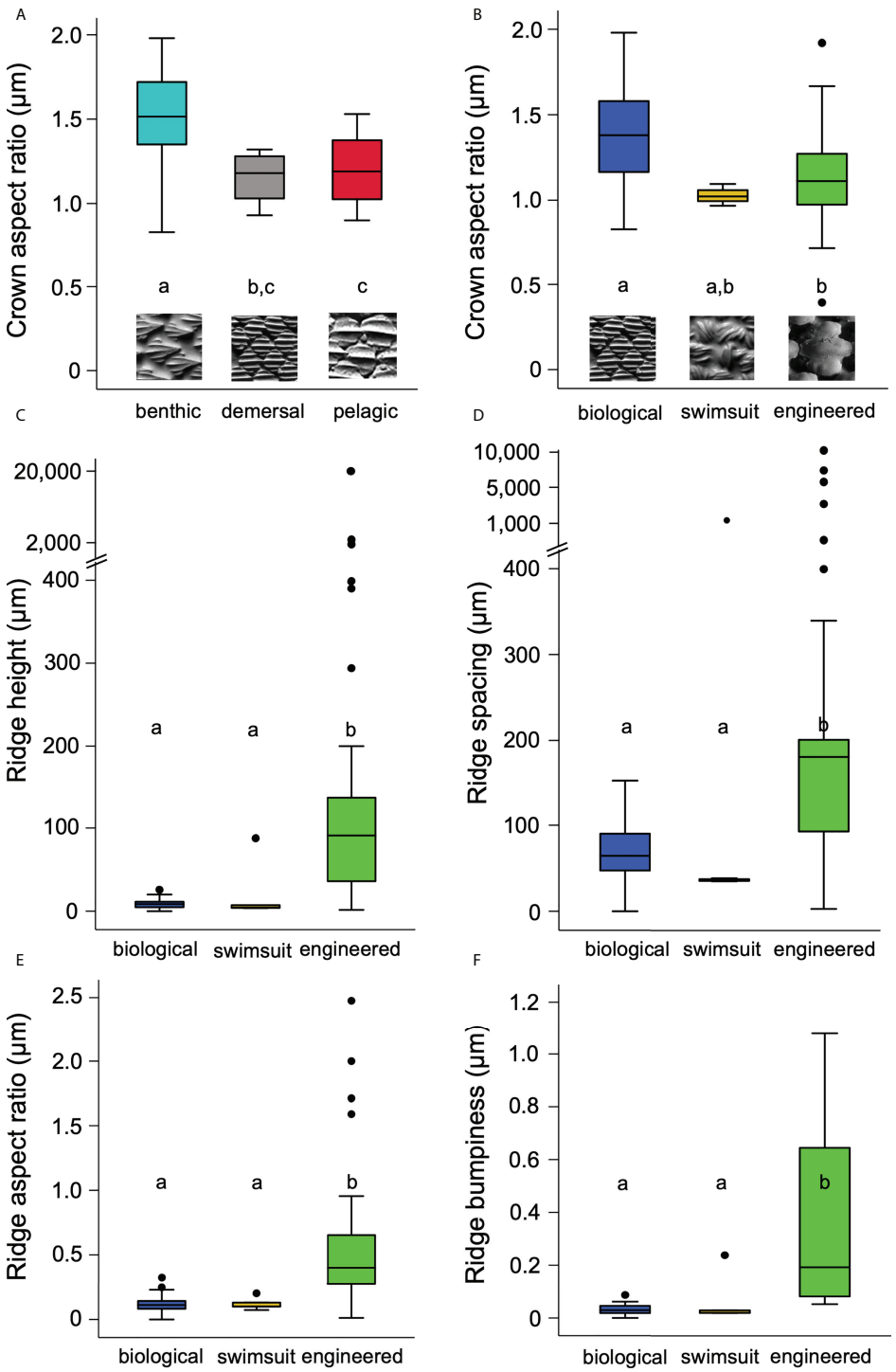

FIGURE 3
Surface characteristics for materials studied. Significant groupings are marked by letters. **(A)** Denticle crown aspect ratio versus the three different habitat groups of sharks. Insets represent one shark species from each habitat group: benthic (chain catshark), demersal (Atlantic sharpnose shark), and pelagic (white shark). **(B)** Crown aspect ratio versus the three types of materials: biological (Atlantic sharpnose shark), swimsuit (Speedo Lzr® Racer Elite 2), and engineered (shark-inspired surface, Domel et al., 2018b). **(C)** Ridge height versus material type. **(D)** Ridge spacing versus types of materials. **(E)** Ridge aspect ratio versus material type. **(F)** Ridge bumpiness versus material type. Note that y-axes in **(C, D)** are broken to display the large denticle ridge height and spacing values.

(mean 1.4 ± 0.04 Bonferroni: $p = 0.04$), while shark skin and swimsuit values (mean 1.0 ± 0.03, Bonferroni: $p = 0.1$) and engineered and swimsuit values were similar (Figure 3B; Table 1, Bonferroni: $p = 1.0$). Mean engineered material ridge height (mean 987.0 ± 738.0 μm) was higher than the other materials (Figure 3C; Table 1, Kruskal-Wallis: $p < 0.001$, engineered-swimsuit Bonferroni: $p < 0.001$, engineered-biological Bonferroni: $p < 0.001$), while swimsuit (mean 21.4 ± 16.6 μm) and shark skin (mean 8.9 ± 0.8 μm) were similar (Bonferroni: $p = 1.0$). Ridge spacing also differed (Kruskal-Wallis: $p < 0.001$): biological shark skin (mean 73.2 ± 5.4 μm) and swimsuit materials (mean 271.0 ± 234.0 μm) were similar (Bonferroni: $p = 0.3$), while engineered material ridge spacing (mean 1031.0 ± 473.0 μm) was higher than the other materials (Figure 3D; Table 1, engineered-biological Bonferroni: $p < 0.001$, engineered-swimsuit Bonferroni: $p = 0.003$). Ridge aspect ratio was higher in engineered materials (mean 0.6 ± 0.1) compared to the other materials (Figure 3E; Table 1, Kruskal-Wallis: $p < 0.001$, engineered-biological Bonferroni: $p < 0.001$, engineered-swimsuit Bonferroni: $p = 0.007$). Ridge bumpiness was similar between the biological shark skin (mean 0.03 ± 0.003) and swimsuit material (mean 0.07 ± 0.04, Kruskal-Wallis: $p < 0.001$, Bonferroni: $p = 1.0$); however, engineered material (mean 0.4 ± 0.1) had higher ridge bumpiness compared to both the shark skin and swimsuits (Figure 3E; Table 1, engineered-biological Bonferroni: $p < 0.001$, engineered-swimsuit Bonferroni: $p = 0.008$).

Discussion

Overall, biomimetic shark skin materials did not closely replicate the surface ornamentation of actual shark skin. Measured three-dimensional (3D) surfaces of engineered riblets differed from shark skin in the height, pattern, and spacing of the ridged surfaces (Figure 2). Most competition swimsuit fabrics more closely matched shark skin surface metrics across the variables measured (Figure 3) but did not possess the distinct parallel longitudinal ridges that are characteristic of shark skin denticles (Figures 2A, B). The many challenges involved in quantifying the complex surface geometry of shark skin and the common use of two-dimensional imaging approaches such as scanning electron microscopy have limited the data available to engineers and swimsuit manufacturers needed to match the 3D surface structure of shark skin.

Surface profilometry techniques have been applied to many biological surfaces, enabling 3D data collection of surface metrics on shark skin (Wainwright et al., 2017; Baeckens et al., 2019; Wainwright et al., 2019; Popp et al., 2020). One advantage of gel-based 3D surface profilometry is that no coating needs to be applied to the surface, the technique is non-destructive, and even reflective or damp surfaces can be imaged with accuracy approaching 1.0 um (Wainwright et al., 2017). However, even with 3D data from shark skin, current manufacturing technology faces challenges in producing engineered surfaces that replicate the intricate details of shark skin surfaces at relevant size scales. Additive manufacturing (3D printing) at resolutions that match the size scale of shark denticles is extremely challenging with current technology, as is the ability to manufacture sufficiently large surface areas with appropriately patterned biologically-sized denticles for testing and application to underwater systems. Due to the overhanging conformation of denticle crowns (Reif, 1985; Motta et al., 2012; Ankhelyi et al., 2018), even molding the shark skin surface does not fully replicate 3D skin surface characteristics.

Riblet structures are well known to reduce drag by altering skin friction at the fluid-surface interface (Bechert and Hage, 2007; Dean and Bhushan, 2010; García-Mayoral and Jiménez, 2011; Raayai-Ardakani and McKinley, 2017; Raayai-Ardakani and McKinley, 2019; Suprapaneni et al., 2022). But to date, both computational and experimental estimates of forces on riblet samples have been conducted on rigid elements, and not on surfaces undergoing rhythmic movement as occurs when the skin surface of sharks oscillates during undulatory locomotion (Lauder et al., 2016). Flow over moving skin surfaces can differ considerably from rigidly mounted surfaces, and engineered surfaces would likely experience improved performance if their surface riblet characteristics more closely matched to those of shark skin.

We noted differences in denticle surface characteristics among the three habitat types that we assigned to each of the 17 shark species studied, suggesting that denticle surface characteristics may be related, at least in part, to mean swimming speeds of sharks (Figures 3A; S1). Some benthic

TABLE 1 Mean surface measurements for each material type ± one standard error.

Material Type	Crown aspect ratio	Ridge height (μm)	Ridge spacing (μm)	Ridge aspect ratio	Ridge bumpiness
Biological	1.4 ± 0.04 (43)[a]	8.7 ± 0.8 (43)[a]	73.2 ± 5.4 (43)[a]	0.1 ± 0.01 (43)[a]	0.03 ± 0.003 (43)[a]
Swimsuit	1.0 ± 0.03 (4)[a,b]	21.4 ± 16.6 (5)[a]	271.0 ± 234.0 (5)[a]	0.1 ± 0.02 (5)[a]	0.1 ± 0.04 (5)[a]
Engineered	1.1 ± 0.1 (16)[b]	987.0 ± 738.0 (27)[b]	1031.0 ± 473.0 (26)[b]	0.6 ± 0.1 (27)[b]	0.4 ± 0.1 (12)[b]

- Numbers in parentheses are sample sizes.
- Columns with different letters are significantly different.

shark species (e.g., chain catshark, *Scyliorhinus retifer*) spend considerable time sedentary on the ocean floor with limited open water locomotion (see Compagno, 2001). Other open ocean pelagic sharks such as the white shark (*Carcharodon carcharias*), which undertake long migrations, are nearly constantly in motion and the skin surface is thus subjected to continuous water flow where drag reduction and reduced energetic costs may be at a premium (Compagno, 2001). Domel et al. (2018b) compared mako shark, white shark, and leopard shark skin surfaces and showed differences in overall surface texture patterning and ridge spacing: mako and white sharks have smaller denticles with small-scale surface ridge patterning compared to leopard sharks. In the current study, we also documented that denticle crown aspect ratios are larger in benthic sharks than in demersal or pelagic species, and pelagic species also tend to have smaller denticle surface ridges which are more tightly packed across the skin surface (Supplemental Tables 1, 2; Figure S1). The functional effect of differences among denticle surface textures that correspond to different shark habitat types is still unknown, and new research is needed to specifically address how different shark surface textures affect drag and lift forces on the skin surface.

Although shark skin surfaces have been shown to increase swimming performance, by both reducing drag and enhancing thrust (Oeffner and Lauder, 2012; Lauder et al., 2016), there are few data published on hydrodynamic flow patterns over shark skin. Du Clos et al. (2018) studied flow patterns over mako shark skin in fixed samples, but flow dynamics over shark skin surfaces moving in a biomimetic undulatory manner remains largely unknown (Anderson et al., 2001). Future experiments measuring flow over shark skin with different surface textures (e.g., Figures 3A, S1), especially under dynamic conditions, will be a key next step in understanding the effect of shark skin-inspired designs on aquatic propulsion.

Data availability statement

The original contributions presented in the study are included in the article/Supplementary Material. Further inquiries can be directed to the corresponding author.

Ethics statement

All work followed institutional ethical guidelines, and valid scientific collecting permits were used to obtain shark tissues.

Author contributions

MG-S and GL conceptualized the project idea. MG-S collected and analyzed the data. MG-S and GL both contributed to the writing of the manuscript. All authors agree to be held accountable for the content herein and approve the final version of the manuscript.

Funding

This work was funded by an NSF PRFB1907211 grant to MG-S, and NSF IOS-2128033 to GL.

Acknowledgments

We would like to thank Diego Bernal at the University of Massachusetts Dartmouth for supplying some of the shark skin tissue and Andrew Williston at the Harvard Museum of Comparative Zoology for help with tissue accession from the ichthyology collection. We would also like to acknowledge Dylan Wainwright, Madeleine Ankhelyi, and Meghan Popp for prior collaborative research that generated some of the GelSight images used for analyses in this paper.

Conflict of interest

The authors declare that the research was conducted in the absence of any commercial or financial relationships that could be construed as a potential conflict of interest.

Publisher's note

Supplementary material

The Supplementary Material for this article can be found online at: https://www.frontiersin.org/articles/10.3389/fmars.2022.975062/full#supplementary-material

References

Anderson, E. J., McGillis, W., and Grosenbaugh, M. A. (2001). The boundary layer of swimming fish. *J. Exp. Biol.* 204, 81–102. doi: 10.1242/jeb.204.1.81

Ankhelyi, M., Wainwright, D. K., and Lauder, G. V. (2018). Diversity of dermal denticle structure in sharks: skin surface roughness and three-dimensional morphology. *J. Morphol.* 279, 1132–1154. doi: 10.1002/jmor.20836

Baeckens, S., Wainwright, D. K., Weaver, J. C., Irschick, D. J., and Losos, J. B. (2019). Ontogenetic scaling patterns of lizard skin surface structure as revealed by gel-based stereo-profilometry. *J. Anat.* 235, 346–356. doi: 10.1111/joa.13003

Bechert, D. W., Bruse, M., and Hage, W. (2000). Experiments with three-dimensional riblets as an idealized model of shark skin. *Exp. Fluids* 28, 403–412. doi: 10.1007/s003480050400

Bechert, D. W., and Hage, W. (2007). "Drag reduction with riblets in nature and engineering," in *In flow phenomena in nature. volume 2. inspiration, learning, and application*. Ed. R. Liebe (Southampton, UK: WIT Press), 457–469.

Bechert, D. W., Hoppe, G., and Reif, W.-E. (1985). On the drag reduction of the shark skin. *AIAA J.* 85-0546 1985, 1–18. doi: 10.2514/6.1985-546

Castro, J. I. (2011). *The sharks of north America* (Oxford: Oxford Univ. Press).

Chamorro, L. P., Arndt, R., and Sotiropoulos, F. (2013). Drag reduction of large wind turbine blades through riblets: Evaluation of riblet geometry and application strategies. *Renewable Energy* 50, 1095–1105. doi: 10.1016/j.renene.2012.09.001

Compagno, L. J. V. (2001). *Sharks of the world: an annotated and illustrated cataglogue of shark species known to date: Bullhead, mackerel and carpet sharks (Heterodontiformes, lamniformes and orectolobiformes)*. Rome:FAO Vol. 2. 1–269.

Dean, B., and Bhushan, B. (2010). Shark-skin surfaces for fluid-drag reduction in turbulent flow: a review. *Philos. Trans. R. Soc. A: Math. Phys. Eng. Sci.* 368, 4775–4806. doi: 10.1098/rsta.2010.0201

Domel, A. G., Domel, G., Weaver, J., Saadat, M., Bertoldi, K., and Lauder, G. V. (2018b). Hydrodynamic properties of biomimetic shark skin: effect of denticle size and swimming speed. *Bioinsp. Biomimet.* 13, 056014. doi: 10.1088/1748-3190/aad418

Domel, A. G., Saadat, M., Weaver, J., Haj-Hariri, H., Bertoldi, K., and Lauder, G. V. (2018a). Shark denticle-inspired designs for improved aerodynamics. *J. R. Soc Inter.* 15, 20170828. doi: 10.1098/rsif.2017.0828

Du Clos, K. T., Lang, A., Devey, S., Motta, P. J., Habegger, M. L., and Gemmell, B. J. (2018). Passive bristling of mako shark scales in reversing flows. *J. R. Soc Inter.* 15, 20180473. doi: 10.1098/rsif.2018.0473

Gabler-Smith, M. K., Wainwright, D. K., Wong, G. A., and Lauder, G. V. (2021). Dermal denticle diversity in sharks: novel patterns on the interbranchial skin. *Int. Org. Biol.* 3, obab034. doi: 10.1093/iob/obab034

García-Mayoral, R., and Jiménez, J. (2011). Drag reduction by riblets. *Phil. Trans. R. Soc A* 369, 1412–1427. doi: 10.1098/rsta.2010.0359

Hutchinson, H. (2008). Beyond the shark skin suit. *Mechanical Eng.* 130, 42.

Ibrahim, M., Amran, S., Yunos, Y., Rahman, M., Mohtar, M., Wong, L., et al. (2018). The study of drag reduction on ships inspired by simplified shark skin imitation. *Appl. Bionics Biomech.* 2018, 1–11. doi: 10.1155/2018/7854321

Laschi, C., Mazzolai, B., Mattoli, V., Cianchetti, M., and Dario, P. (2009). Design of a biomimetic robotic octopus arm. *Bioinsp. Biomimet.* 4, 015006. doi: 10.1088/1748-3182/4/1/015006

Lauder, G. V., Wainwright, D. K., Domel, A. G., Weaver, J., Wen, L., and Bertoldi, K. (2016). Structure, biomimetics, and fluid dynamics of fish skin surfaces. *Phys. Rev. Fluids* 1, 060502. doi: 10.1103/PhysRevFluids.1.060502

Leitl, P. A., Stenzel, V., Flanschger, A., Kordy, H., Feichtinger, C., Kowalik, Y., et al. (2020). "Riblet surfaces for improvement of efficiency of wind turbines," in *AIAA scitech 2020 forum*. Orlando FL:American Institute of Aeronautics and Astronautics, Inc., 0308.

Margheri, L., Laschi, C., and Mazzolai, B. (2012). Soft robotic arm inspired by the octopus: I. from biological functions to artificial requirements. *Bioinsp. Biomimet.* 7, 025004. doi: 10.1088/1748-3182/7/2/025004

Motta, P., Habegger, M. L., Lang, A., Hueter, R., and Davis, J. (2012). Scale morphology and flexibility in the shortfin mako isurus oxyrinchus and the blacktip shark carcharhinus limbatus. *J. Morphol.* 273, 1096–1110. doi: 10.1002/jmor.20047

Oeffner, J., and Lauder, G. V. (2012). The hydrodynamic function of shark skin and two biomimetic applications. *J. Exp. Biol.* 215, 785–795. doi: 10.1242/jeb.063040

Popp, M., White, C. F., Bernal, L. P., Wainwright, S. A., and Lauder George, V. (2020). The denticle surface of thresher shark tails: three-dimensional structure and comparison to other pelagic species. *J. Morphol.* 281, 938–955. doi: 10.1002/jmor.21222

Raayai-Ardakani, S., and McKinley, G. H. (2017). Drag reduction using wrinkled surfaces in high reynolds number laminar boundary layer flows. *Phys. Fluids* 29, 093605. doi: 10.1063/1.4995566

Raayai-Ardakani, S., and McKinley, G. H. (2019). Geometric optimization of riblet-textured surfaces for drag reduction in laminar boundary layer flows. *Phys. Fluids* 31, 053601. doi: 10.1063/1.5090881

R Core Team (2020). *R: a language and environment for statistical computing* (Vienna, Austria: R Foundation for Statistical Computing). Available at: https: www.R-project.org/.

Reif, W.-E. (1985). Squamation and ecology of sharks. *Cour. Forsch.-Inst. Senckenberg*. Frankfurt am Main 78, 1–255.

Sareen, A., Deters, R. W., Henry, S. P., and Selig, M. S. (2014). Drag reduction using riblet film applied to airfoils for wind turbines. *J. Solar Energy Eng.* 136, 1–19. doi: 10.1115/1.4024982

Suprapaneni, V. A., Schindler, M., Ziege, R., de Faria, L. C., Wölfer, J., Bidan, C. M., et al. (2022). Groovy and gnarly: Surface wrinkles as a multifunctional motif for terrestrial and marine environments. *Int. Comp. Biol.*, icac079. doi: 10.1093/icb/icac079

Takagi, H., and Sanders, R. (2000). Hydrodynamics makes a splash. *Phys. World* 13, 39. doi: 10.1088/2058-7058/13/9/30

Wainwright, D. K., Fish, F. E., Ingersoll, S., Williams, T. M., St. Leger, J., Smits, A. J., et al. (2019). How smooth is a dolphin? *Ridged Skin Odontocetes. Biol. Let.* 15, 20190103. doi: 10.1098/rsbl.2019.0103

Wainwright, D. K., and Lauder, G. V. (2016). Three-dimensional analysis of scale morphology in bluegill sunfish, lepomis macrochirus. *Zoology* 119, 182–195. doi: 10.1016/j.zool.2016.02.006

Wainwright, D. K., and Lauder, G. V. (2018). "Mucus matters: the slippery and complex surfaces of fish," in *Functional surfaces in biology III*. Eds. E. Gorb and S. Gorb (Berlin: Springer Verlag), 223–246.

Wainwright, D. K., Lauder, G. V., and Weaver, J. C. (2017). Imaging biological surface topography *in situ* and *in vivo*. *Methods Ecol. Evol.* 8, 1626–1638. doi: 10.1111/2041-210X.12778

Wen, L., Weaver, J. C., and Lauder, G. V. (2014). Biomimetic shark skin: design, fabrication, and hydrodynamic function. *J. Exp. Biol.* 217, 1656–1666. doi: 10.1242/jeb.097097

White, C. H., Lauder, G. V., and Bart-Smith, H. (2021). Tunabot flex: a tuna-inspired robot with body flexibility improves high-performance swimming. *Bioinsp. Biomimet.* 16, 026019. doi: 10.1088/1748-3190/abb86d

Winter, A. G., and Hosoi, A. E. (2011). Identification and evaluation of the Atlantic razor clam (Ensis directus) for biologically inspired subsea burrowing systems. *Int. Comp. Biol.* 51, 151–157. doi: 10.1093/icb/icr038

Xie, Z., Domel, A. G., An, N., Green, C., Gong, Z., Wang, T., et al. (2020). Octopus arm-inspired tapered soft actuators with suckers for improved grasping. *Soft Robotics* 7, 639–648. doi: 10.1089/soro.2019.0082

Zhao, D.-Y., Huang, Z.-P., Wang, M.-J., Wang, T., and Jin, Y. (2012). Vacuum casting replication of micro-riblets on shark skin for drag-reducing applications. *J. Mater. Process. Technol.* 212, 198–202. doi: 10.1016/j.jmatprotec.2011.09.002

Zhu, J., White, C., Wainwright, D. K., Di Santo, V., Lauder, G. V., and Bart-Smith, H. (2019). Tuna robotics: A high-frequency experimental platform exploring the performance space of swimming fishes. *Sci. Robotics* 4, eaax4615. doi: 10.1126/scirobotics.aax4615